

Electronic Supporting Information

For

A Dual-Fluorescent Nano-Carrier for Delivering Photoactive Ruthenium  
Polypyridyl Complex

**Content**

**Figure S1.**  $^1\text{H}$ -NMR spectrum of  $[\text{Ru}(\text{bpy})_2(\text{dmbpy})]\text{Cl}_2$ .

**Figure S2.** ESI-MS spectrum of **Ru-1**.

**Table S1.** The size distribution and zeta-potential of nanoparticles.

**Figure S3.** Photos of Ru-HSA-UCNPs before and after centrifugation.

**Table S2.** The Ru-1 loading efficiency results.

**Figure S4.** XRD patterns of the NaYF<sub>4</sub>: 20% Yb, 0.5% Tm nanoparticles.

**Figure S5.** MTT assay.

**Figure S6.** Cellular uptake of ruthenium complexes.

**Figure S7.** Cellular uptake of Ru loaded HSA nanoparticles.

**Figure S8.** Cytotoxicity assay of ruthenium complexes and their conjugates of UCNPs.

**Figure S9.** The fluorescence emission spectrum of Ru-HSA-UCNPs at 450 nm excitation.

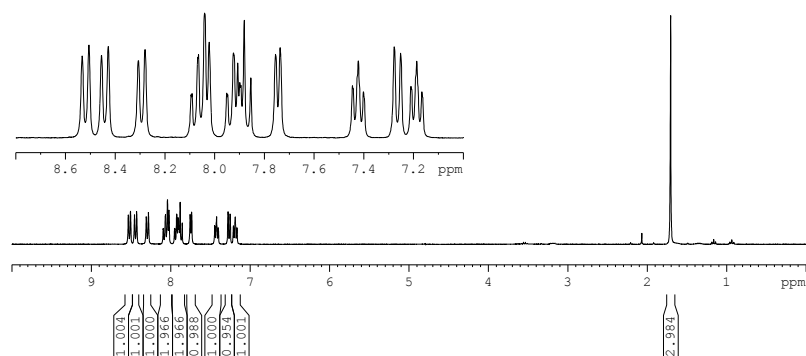


**Figure S1.**  $^1\text{H-NMR}$  spectrum of  $[\text{Ru}(\text{bpy})_2(\text{dmbpy})]\text{Cl}_2$  in  $\text{D}_2\text{O}$ . The spectrum was recorded using presaturation pulse sequence to suppress the residual HDO signal. The 1.705 ppm peak of the methyl signal from the 6,6'-dimethyl-2,2'-bipyridine. All of 11 unique signals from aromatic group were observed in consideration of the symmetry of the complex. (two of which are overlapping).

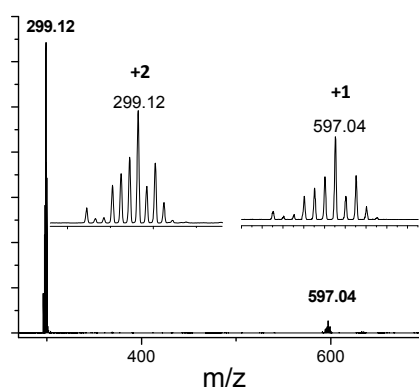


**Figure S2.** Identification of **Ru-1** by ESI-MS. The spectrum was measured in the positive mode. Composition:  $\text{RuC}_{32}\text{H}_{28}\text{N}_6$ , measured ESI-MS spectrum:  $m/z = 597.04$ ,  $z = 1$ ;  $m/z = 299.12$ ,  $z = 2$ ; theoretically calculated isotope pattern,  $m/z = 596.67$ ,  $z = 1$ ,  $m/z = 298.84$ ,  $z = 2$ .

**Table S1.** The size distribution and zeta-potential of free UCNPs, HSA-UCNPs and Ru-HSA-UCNPs.

	Free UCNPs	HSA-UCNPs	Ru-HSA-UCNPs
Size (nm)	60	105	120
PDI	0.16	0.068	0.092
Zeta-potential	+5	-20.3	-45.3

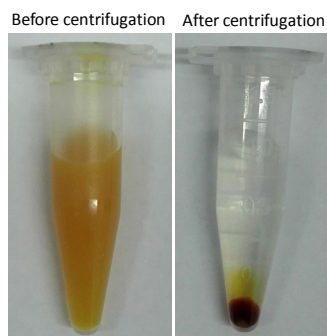


**Figure S3.** Photos of Ru-HSA-UCNPs before and after centrifugation. The Ru-HSA-UCNPs were dispersed in water showing deep yellow solution. The Ru-1 was completely co-precipitation after 15000 rpm centrifugation for 10 min. The precipitation were resuspended after sonication dispersion.

**Table S2.** The Ru-1 loading efficiency measurement.

Amount ( $\mu\text{mol}$ )	1	2	3	4
Loading efficiency (%)	76.7	70.7	66.9	56.5

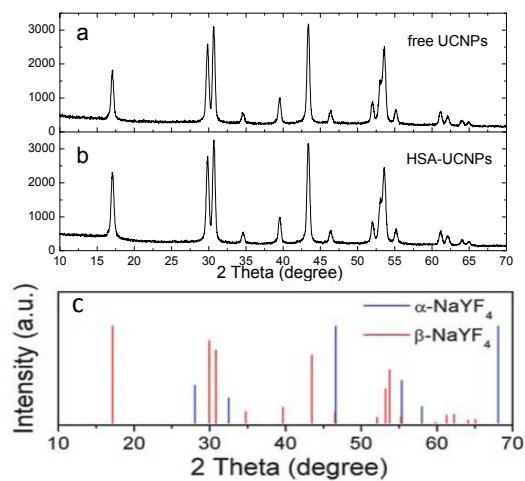


**Figure S4.** XRD patterns of the  $\text{NaYF}_4$ : 20% Yb, 0.5% Tm nanoparticles. a) free UCNPs. b) HSA-UCNPs. c) the calculated line patterns of  $\alpha\text{-NaYF}_4$  and  $\beta\text{-NaYF}_4$ .

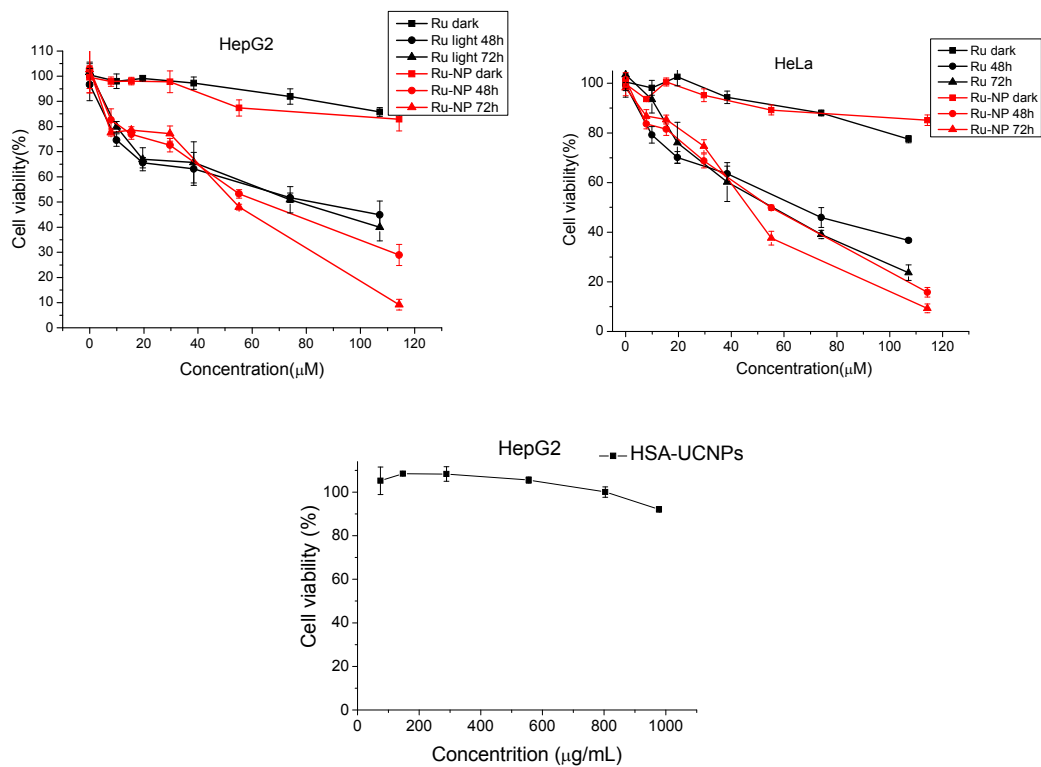


**Figure S5.** MTT assay of Ru-1, photoactivated Ru-1 on HepG2 and HeLa cells. MTT assay of HSA-UCNPs on HepG2 cells.

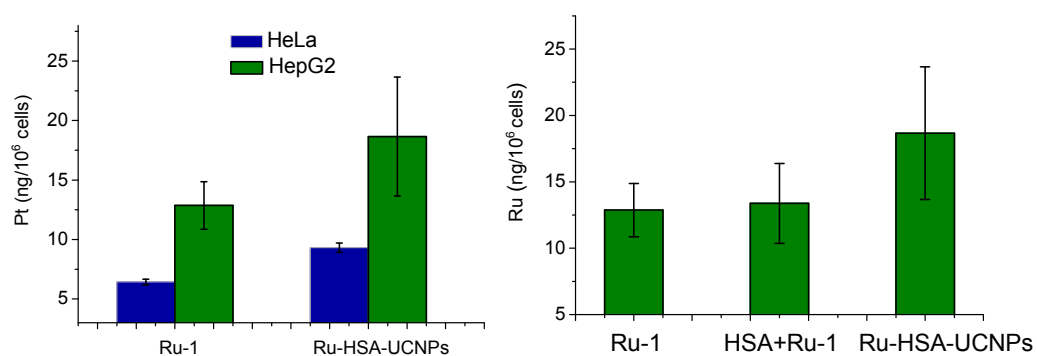


**Figure S6.** Cellular uptake of ruthenium complexes. (A) The comparison of cellular uptake of **Ru-1** and Ru-HSA-UCNPs on HepG2 cells and HeLa cells. (B) The comparison of cellular uptake of **Ru-1**, HSA + **Ru-1**, Ru-HSA-UCNPs on HepG2 cells. Cells were treated with same ruthenium concentration of 100  $\mu\text{M}$  for 4 hours. The accumulation of ruthenium in cells was measured by ICP-MS.

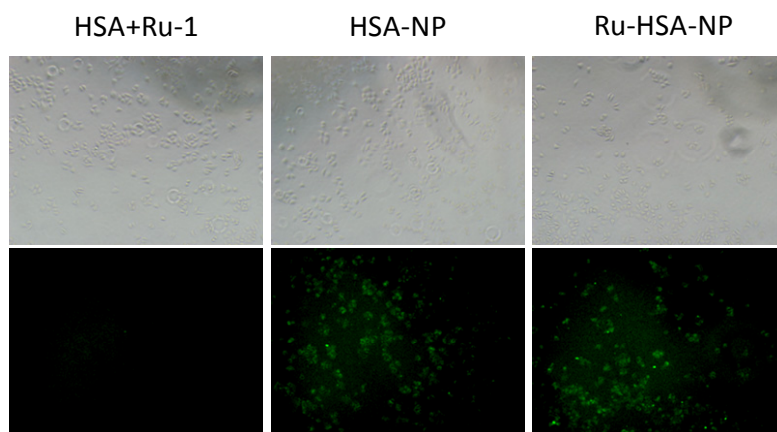


**Figure S7.** The cellular uptake of HSA and nanoparticles. The cells were treated with HSA protein + **Ru-1**, polymerized HSA nanoparticles (HSA-NP), and **Ru-1** loaded HSA-NP (Ru-HSA-NP) for 4 h on HepG2 cells. The fluorescence images were measured by fluorescence microscopy.

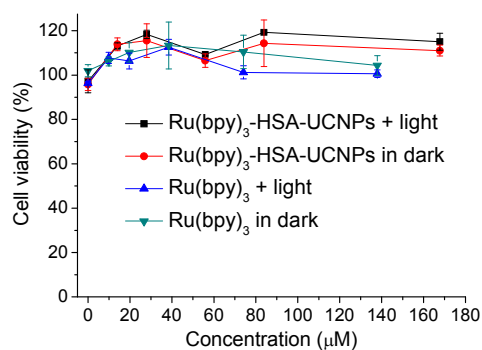


**Figure S8.** Cytotoxicity assay of free  $[\text{Ru}(\text{bpy})_3]^{2+}$  and its conjugates of HSA-UCNPs ( $\text{Ru}(\text{bpy})_3\text{-HSA-UCNPs}$ ). The cell viability was measured on HepG2 cells with the treatment of ruthenium compounds with light irradiation (in  $10 \text{ mW cm}^{-2}$  irradiation power density) for 10 min or in dark.

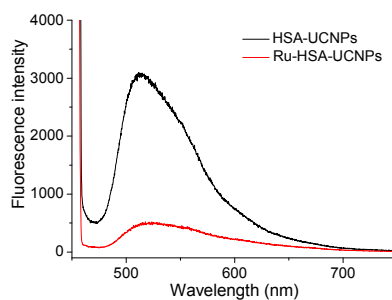


**Figure S9.** The fluorescence emission spectra of HSA-UCNPs and Ru-HSA-UCNPs. The fluorescence spectra were measured at 450 nm excitation.